Wake Density and Temperature

Axial results

Of all the laws governing the wakes, the growth law is certainly the best established one. As the wake growth is faster for turbulent than for laminar wakes, the density $[(\rho_\infty - \rho_0)/\rho_\infty]$ and temperature $[(T_0 - T_\infty)/T_\infty]$ defects diffuse or decrease more rapidly in turbulent than in laminar wakes; graphical presentations of this decrease vs downstream distance have been presented by Demetriades.[9] In Fig. 3, the normalized density and temperature defects are given. For the density data, slopes of 0.09, 0.32, and 0.36 are found respectively for 1.0, 5.0, and 7.6 torr, and for the temperature defects, the slopes found are 0.42, 1.00, and 1.46 for 1.0, 5.0, and 7.6 torr. The temperature data given here are obtained by inverting the density data, since, according to Lykoudis,[10] the pressure will be nearly ambient at a downstream distance X/D approximately equal to $M^2/9$; in our case, this distance is 25 X/D, so the hypothesis of an isobaric wake is justified. The marked difference between the density and temperature decay rates is to be expected as a result of the form of the equation of state in the hypothesis of an isobaric wake as pointed out by Demetriades.[9]

Radial results

The radial variation of the density form parameter $[(\rho_\infty - \rho)/(\rho_\infty - \rho_0)]$ can be compared with the density results computed by Wen.[11] As the density distribution is not gaussian while the temperature is, it is more interesting to compute wake temperature from the density data assuming an isobaric wake. All the temperature data so obtained can be fitted by a gaussian distribution which shows good agreement with Wen's results. Moreover all the distributions curves obtained at several distances in the wake can be used to produce a complete map of the average temperature of the wake represented by the carpet plot of Fig. 4. The first part of the wake extending up to 150 body diams is fitted by a gaussian radial distribution and a constant value along the wake axis. Beyond that point, the radial gaussian distribution is retained and the axial data is fitted by an exponential decay of temperature.

Concluding Remarks

The free flight range facility has shown great potentiality for wake studies behind hypersonic models. However this facility provides data which are often statistically poor because of the limited number of firings observed and of the short observation time available on each firing. This is particularly true for the large size models required to develop a turbulent wake at an ambient pressure not exceeding 10 torr. Evidently our data suffer from this drawback since only 4 firings at 1.0 torr and 7 at 7.6 torr were made available.

References

[1] Muntz, E. P., "Static Temperature Measurements in a Flowing Gas," *The Physics of Fluids*, Vol. 5, No. 1, Jan. 1962, pp. 80–90.

[2] Muntz, E. P. and Softley, E. S., "A Study of Laminar Near Wakes," *AIAA Journal*, Vol. 4, No. 6, June 1966, pp. 961–968.

[3] Rothe, D. E., "Electron Beam Studies of the Diffusive Separation of Helium-Argon Mixtures," *The Physics of Fluids*, Vol. 9, No. 9, Sept 1966, pp. 1643–1658.

[4] Dionne, J. G. G. et al., "Mass Density Measurements in Hypersonic Wakes," *AGARD Conference Proceedings No. 19, Fluid of Physics of Hypersonic Wakes*, Colorado State Univ., May 1967.

[5] Tardif, L. and Dionne, J. G. G., "Density Distribution in Turbulent and Laminar Wakes," *AIAA Journal*, Vol. 6, No. 10, Oct. 1968, pp. 2027–2029.

[6] Davidson, G. and O'Neill, R., "The Fluorescence of Air and Nitrogen Excited by 50 Kev Electrons," AFCRL-64-466, May 1964, Air Force Cambridge Research Lab, Bedford, Mass.

[7] Camac, M., "Boundary Layer Measurements with an Electron Beam," Research Report 275, 1967, AVCO Everett, Everett, Mass.

[8] Robertson, W. J., "The Effect of Reflected Shock System on Hypersonic Wakes," TN/1846/69, 1969 Defence Research Establishment Valcartier, Quebec, Canada.

[9] Demetriades, A., "Mean-Flow Measurements in an Axisymmetric Compressible Turbulent Wake," *AIAA Journal*, Vol. 6, No. 3, March 1968, pp. 432–439.

[10] Lykoudis, P. S., "A Review of Hypersonic Wake Studies," *AIAA Journal*, Vol. 4, No. 4, April 1966, pp. 577–590.

[11] Wen, K. S., Chen, T., and Lieu, B., "A Theoretical Study of Hypersonic Sphere Wakes in Air and Comparisons with Experiments," AIAA Paper 68-703, Los Angeles, Calif., June 1968.

Observations of Surface Ablation Patterns in Subliming Materials

A. L. Laganelli* and R. E. Zempel†

General Electric Company, Valley Forge, Pa.

Introduction

THE discovery of surface ablation patterns on ground test models as well as recovered flight vehicles, with the subsequent conjectures explaining the phenomena, has been an item of interest over the past few years. A comprehensive review of the subject matter (up through mid-1968) can be found in a paper by Laganelli and Nestler.[1] Several additional investigations concerning the phenomena consist of the theoretical analyses of Donaldson,[2] Lew and Li,[3] Inger,[4] Tobak,[5] Nachtsheim,[6] Person,[7] and Probstein and Gold[8] as well as the experimental results of Williams.[9]

The present study consisted of investigating surface ablation patterns as developed by natural ablation and by introducing disturbances on the body. The test program was conducted in the NASA Langley 8-Ft High-Temperature Structures Tunnel. The facility provides a nominal free-stream Mach number of 7.4, stagnation temperature up to 3500°R, and stagnation pressure range from 1000 to 2800 psia. The experimental models consisted of sharp-tipped Teflon cones with a base diameter of approximately 30 in. and a half-angle of 36°. The actual test matrix conducted in the Langley facility consisted of many tests whose results would be beyond the scope of this Note. These tests included single and multiple rows and columns of drilled holes and pins at various longitudinal and lateral spacings and depths, random-spaced holes, logarithmic-spaced holes, slots, steps, dissimilar materials, and angle-of-attack effects. Several of the more pertinent features of the tests will be reported, and interested readers can find specific details in Ref. 2. Preliminary tests were made to confirm local pressure predictions and to indicate what test exposure time was required to produce the patterns. The results of these tests are reported in Ref. 1.

Test Results

Inasmuch as the test time for the Langley facility was limited (30 secs) it was decided to reablate one of the preliminary models (shown in Fig. 1) to simulate longer ablation time. The results of this test are shown in Fig. 2. It is observed that the longer ablation time appeared to produce

Received April 17, 1970; revision received May 27, 1970. The authors wish to acknowledge the U.S. Air Force who sponsored this work under Contract AF-04(694)914. Also, the authors thank D. E. Nestler who supervised much of the work and S. Stadelmeier for his photographic and measurement techniques.

* Research Engineer, Aerothermodynamics Re-entry and Environmental Systems Division. Member AIAA.

† Research Engineer, Aerothermodynamics, Re-entry and Environmental Systems Division.

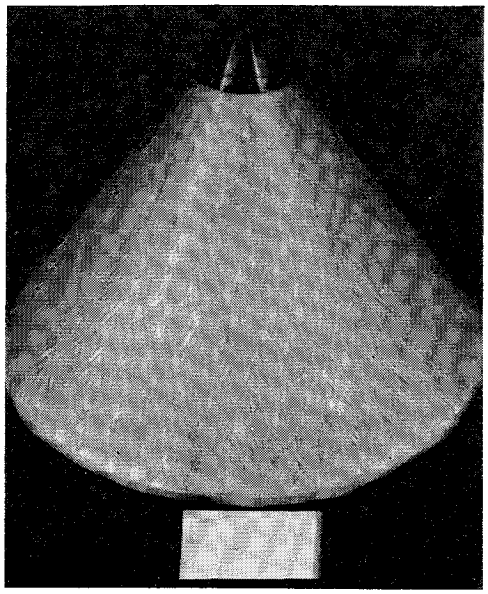

Fig. 1 Teflon 36° half-angle sharp steel-tip cone; exposure: 23 sec. (Model was photographed with a "rubbing" of the patterns on tracing paper to accentuate the pattern characteristics.[1])

patterns which resembled a more uniform matrix as seen on other ground test models and recovered flight vehicles. A close comparison of the tracings before and after reablation showed that several divider shape patterns‡ that were present in Fig. 1 are still identifiable, yet have coalesced within the diamond-pattern matrix. Although the features of the divider pattern remain, its identity is a regular feature of the entire pattern structure, and the trailing groove no longer exists. It appears that, although ablation itself is not the cause of the patterns, the amount of ablation seems to be quite significant relative to the pattern depth and uniformity over the model surface. Estimates of pattern depth are typically 10% of the total amount of surface recession.

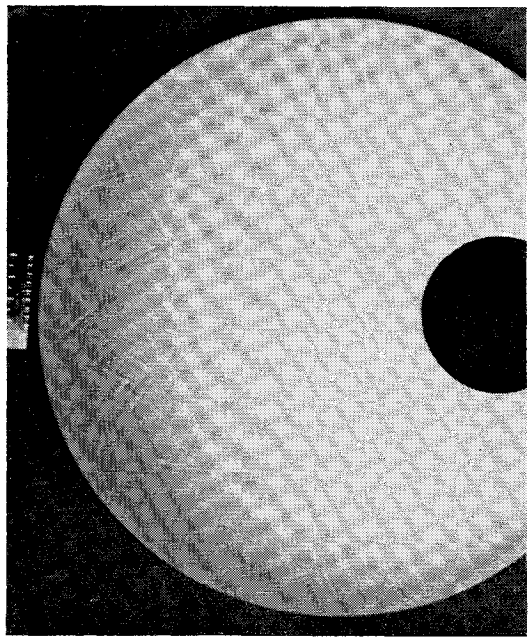

Fig. 2 Reablated Teflon cone model of Fig. 1; total exposure: 53 sec.

‡ A description of the divider shape pattern as well as the mechanism causing its occurrence is given in Ref. 1.

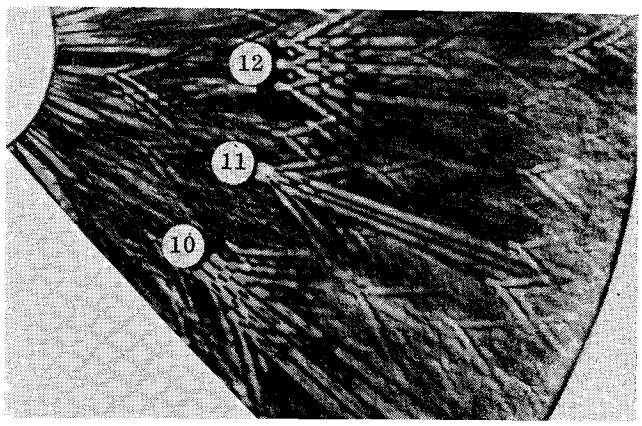

Fig. 3 Tracing of pattern results from disturbances induced circumferentially on Teflon cone; exposure: 23 sec.

Since impact cavities caused by tunnel debris were responsible for the divider shape pattern, induced disturbances were located in the models shown in Figs. 3 and 4. A series of holes were placed in both the circumferential (Fig. 3) and longitudinal directions (Fig. 4) whose spacings were equal to, twice, and half the "natural" transverse (3.8 in.) and longitudinal ($\frac{3}{4}$ in.) wavelengths observed in previous tests. In Fig. 3, location 10 represents three $\frac{1}{8}$-in. diam holes spaced at the natural transverse wavelength. The patterns continued to propagate at the typical $\frac{3}{8}$-in. transverse spacing and typical $\frac{3}{4}$–$\frac{7}{8}$-in. longitudinal spacing for several wavelengths in the stream direction. In location 11, where the hole spacing was half the natural spacing, the patterns diverged to the natural transverse spacing while maintaining the typical longitudinal wavelength. However, the number of cycles was less than the previous case. In location 12, where the hole spacing was twice the natural spacing, the patterns tended to converge to the natural transverse spacing (within two wavelengths). As in the natural spacing case, the patterns persisted several wavelengths downstream while maintaining the typical $\frac{3}{4}$–$\frac{7}{8}$-in. longitudinal spacing. Figure 4 represents a repeat of the previous test but in the longitudinal direction. In location 1, a series of $\frac{1}{16}$-in. diam holes were drilled $\frac{3}{4}$-in. apart along a meridian. The disturbances developed a "fish-bone" pattern that persisted a few wavelengths beyond the last hole. It was noted that no new grooves developed between the hole locations. In location 2, the streamwise spacing of holes was half the natural spacing. The natural spacing appeared to develop weakly between the holes, and more strongly after the last hole location for two wavelengths. In location 3, the hole spacing was twice the natural spacing. It is observed that wave pairs

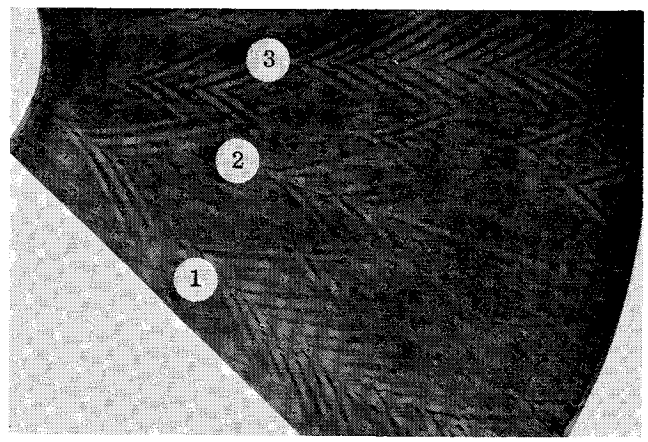

Fig. 4 Tracing of pattern results from disturbances induced longitudinally on Teflon cone; exposure: 23 sec.

developed in between the hole locations at the natural spacing, and a natural wave family also persisted downstream of the holes.

Probable Causes of Surface Pattern Mechanism

A detailed listing of ablation pattern observations is given in tabular form by Laganelli and Nestler[1] with a statement of possible inference that each observation suggests regarding the pattern formation mechanism. The authors suggest a potential relationship between longitudinal vorticity and the diamond-shape pattern which has been explored in Refs. 5 and 7. On the other hand, the periodic behavior of the pattern phenomenon suggests a preferred modal or resonant condition resulting from the fluctuating components in a turbulent flow which was the subject of the investigations in Refs. 2–4, 6, and 8. The experimental results of Ref. 10 would tend to give support to this argument where the pattern wavelength was observed to change during the test. Further support was observed in the Langley tests where induced disturbances at half and twice the natural wavelength developed patterns which diverged and converged, respectively, to their natural mode. It should be noted that the analytical concepts require the existence of vorticity to initiate the modal response or pressure waves from disturbances. Furthermore, it has been observed that the transverse wavelength of longitudinal grooves (preceding diamond patterns) as developed from various vortex generating mechanisms has typically the same value as the diamond pattern. The spacing ratio λ/δ appears to be in good agreement with the range of λ/δ for longitudinal vortices; hence, the significant role of longitudinal vorticity in diamond-pattern development is suggested.

It has been mentioned that although ablation is not a necessary requisite for pattern development, it is required for the patterns to enhance their features in a responding surface. An ablation age parameter,[11] defined as the ratio of the amount of material ablated to the boundary-layer thickness ($\Delta y/\delta$) appears to approach unity for the diamond-shaped patterns to develop in a uniform, symmetric matrix. This phenomenon was observed on the test cones (Figs. 2 and 3), recovered flight vehicles, and several of the rocket exhaust models of Ref. 1 which exhibited an ablation age parameter 0.4.

References

[1] Laganelli, A. L. and Nestler, D. E., "Surface Ablation Patterns—A Phenomenology Study," *AIAA Journal*, Vol. 7, No. 7, July 1969, pp. 1319–1325.

[2] *RVTO Roll Phenomenology Final Report*, CCN-14, Vol. 2, US Air Force Contract AF-04(694)914, General Electric Document 68SD809, July 1968.

[3] Lew, H. G. and Li, H., "The Role of the Turbulent Viscous Sublayer in the Formation of Surface Patterns," TIS-R68SD12, Aug. 1968, General Electric.

[4] Inger, G. R., "Discontinuous Supersonic Flow Past an Ablating Wavy Wall," Document DAC-62375, Sept. 1968, McDonnel-Douglas Corp.

[5] Tobak, M., "Hypothesis for the Origin of Cross-Hatching," *AIAA Journal*, Vol. 8, No. 2, Feb. 1970, pp. 330–334.

[6] Nachtsheim, P. R., "Analysis of the Stability of a Thin Liquid Film Adjacent to a High-Speed Gas Stream," TN-D-4976, Jan. 1969, NASA.

[7] Person, L. N., "Streamwise Directed Vortices and Cross-Hatched Surfaces of Re-entry Vehicles," *Journal of Spacecraft and Rockets*, Vol. 7, No. 1, Jan. 1970, pp. 108–110.

[8] Probstein, R. F., and Gold, H., "Cross-Hatching: A Material Response Phenomena," *AIAA Journal*, Vol. 8, No. 2, Feb. 1970, pp. 364–366.

[9] Williams, E. P., "Experimental Studies of Ablation Surface Patterns and Resulting Roll Torques," AIAA Paper 69-180, New York, 1969.

[10] Larson, H. K. and Mateer, G. G., "Cross-Hatching—A Coupling of Gas Dynamics with the Ablation Process," AIAA Paper 68-670, Los Angeles, 1968.

[11] Donaldson, C. DuP., private communication, Sept. 1968.

Shapes of Missiles of Minimum Ballistic Factor

S. C. JAIN* AND V. B. TAWAKLEY†

Defence Science Laboratory, Delhi, India

A KEEN interest has been shown by a number of authors on the problem of determination of slender axisymmetric power law bodies having minimum ballistic factor. Berman[1] studied the problem for given values of body length, diameter, and specific weight and compared the ballistic coefficient (reciprocal of ballistic factor) of the body with that of a sharp cone having the same dimensions. He employed wind-tunnel measurements and calculated the ratio of ballistic coefficient of the power law body to that of the sharp cone from an empirical variation of drag coefficient with power law exponent. He concluded that the maximum ballistic coefficient of the body can be increased by about 40% over that for a cone if the power law exponent has a value of 0.62. Fink[2] studied the same problem analytically employing the Newtonian theory as well as Newton-Busemann centrifugal theory and compared his results with those of Berman. But in Fink's theory no account was taken of the frictional effects. Miele and Huang[3] considered the effect of skin friction but only employed the Newtonian theory. In this Note the authors have used the more realistic Newton-Busemann centrifugal law and have compared their results with those of Miele and Huang. Earlier results[1–3] follow as particular cases of our analyses.

The ballistic factor of a missile of given length, thickness, and specific weight is proportional to the quality coefficient

$$I = I_1/I_2 \tag{1}$$

where I_1 and I_2 denote the integrals associated with drag and volume of the missile.

The general expression for the drag of a body in hypersonic flow at zero angle of attack when the surface-averaged skin-friction coefficient is constant is given by[4]

$$\frac{D}{4\pi q} = \int_0^l y\left(\dot{y}^3 + k\,\frac{y\dot{y}\ddot{y}}{2} + \frac{c_f}{2}\right)dx \tag{2}$$

where k is a factor equal to zero for Newtonian law and equal to unity for Newton-Busemann law.

The volume of the body is given by

$$V = \pi\int_0^l y^2 dx \tag{3}$$

We now investigate the power law bodies described by

$$y = (d/2)(x/l)^n \tag{4}$$

From Eqs. (2–4), we have

$$I_1 = \frac{4Dl^2}{\pi q d^4} = \frac{2n^3 + k(n^3 - n^2)}{4(2n-1)} + \frac{\alpha^3}{(n+1)} \tag{5}$$

$$I_2 = 4V/\pi d^2 l = 1/(2n+1) \tag{6}$$

where

$$\alpha = (4C_f)^{1/3}(l/d)$$

Therefore the 'quality coefficient' from Eq. (1) becomes

$$I = (2n+1)\left[\frac{2n^3 + k(n^3 - n^2)}{4(2n-1)} + \frac{\alpha^3}{(n+1)}\right] \tag{7}$$

Received January 19, 1970; revision received May 11, 1970. The authors acknowledge their thanks to R. R. Aggarwal for helpful discussions and to the Director, Defence Science Laboratory for permission to publish this work.

* Senior Scientific Assistant, Applied Mathematics Division. Member AIAA.

† Senior Scientific Officer, Applied Mathematics Division.